AD-A065 259   PHOTOMETRICS INC   LEXINGTON MASS   F/G 4/1
                DENSITOMETRIC ANALYSES TO DETERMINE ARTIFICIAL CLOUD EXPANSION --ETC(U)
                MAR 78   C A TROWBRIDGE   F19628-75-C-0126
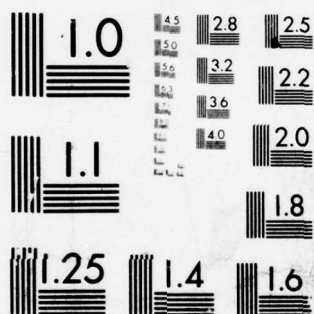UNCLASSIFIED   PHM-05-78   AFGL-TR-78-0075   NL

END
DATE
FILMED

4 --79
DDC

MICROCOPY RESOLUTION TEST CHART

NATIONAL BUREAU OF STANDARDS-1963-A

AFGL-TR-78-0075

LEVEL (13)

DENSITOMETRIC ANALYSES TO DETERMINE ARTIFICIAL
CLOUD EXPANSION CHARACTERISTICS

Christian A. Trowbridge

PhotoMetrics, Inc.
442 Marrett Road
Lexington, Massachusetts 02173

15 March 1978

Final Report for Period 15 February 1978 - 14 February 1978

Prepared for

AIR FORCE GEOPHYSICAL LABORATORY
AIR FORCE SYSTEMS COMMAND
UNITED STATES AIR FORCE
HANSCOM AFB, MASSACHUSETTS 01731

79 03 02 014

REPORT DOCUMENTATION PAGE		READ INSTRUCTIONS BEFORE COMPLETING FORM
1. REPORT NUMBER AFGL-TR-78-0075	2. GOVT ACCESSION NO.	3. RECIPIENT'S CATALOG NUMBER
4. TITLE (and Subtitle) DENSITOMETRIC ANALYSES TO DETERMINE ARTIFICIAL CLOUD EXPANSION CHARACTERISTICS		5. TYPE OF REPORT & PERIOD COVERED Final Report. 15 Feb 1975 — 14 Feb 1978
		6. PERFORMING ORG. REPORT NUMBER PhM-05-78
7. AUTHOR(s) Christian A. Trowbridge		8. CONTRACT OR GRANT NUMBER(s) F19628-75-C-0126
9. PERFORMING ORGANIZATION NAME AND ADDRESS PhotoMetrics, Inc. 442 Marrett Road Lexington, Massachusetts 02173		10. PROGRAM ELEMENT, PROJECT, TASK AREA & WORK UNIT NUMBERS 62101F 669007AC
11. CONTROLLING OFFICE NAME AND ADDRESS Air Force Geophysical Laboratory Hanscom AFB, Massachusetts 01731 Monitor/S.P. Zimmerman/LKB		12. REPORT DATE 15 March 1978
		13. NUMBER OF PAGES 24
14. MONITORING AGENCY NAME & ADDRESS(if different from Controlling Office)		15. SECURITY CLASS. (of this report) Unclassified
		15a. DECLASSIFICATION/DOWNGRADING SCHEDULE

16. DISTRIBUTION STATEMENT (of this Report)

Approved for public release; distribution unlimited.

17. DISTRIBUTION STATEMENT (of the abstract entered in Block 20, if different from Report)

18. SUPPLEMENTARY NOTES

19. KEY WORDS (Continue on reverse side if necessary and identify by block number)
Turbulence
Atmospheric Heating
Turbulent Diffusivity
Fourier Analysis
Reduction of Photographic Images

20. ABSTRACT (Continue on reverse side if necessary and identify by block number)

A program of microdensitometric reduction and computer analysis of photographic images of smoke and chemical tracers in the stratosphere and upper atmosphere is described. Turbulent heating rates, diffusion coefficients and other parameters of turbulence were determined by Fourier and statistical analysis of digitally recorded optical density distributions. →next page

DD $_{1 \text{ JAN } 73}^{\text{FORM}}$ 1473   EDITION OF 1 NOV 65 IS OBSOLETE

19. Key Words (continued)

Chemical Releases
Smoke Trails
Stratosphere
Upper Atmosphere

20. Abstract (continued)

Wind data derived by the smoke trail method in the
stratosphere and mesosphere was also analyzed to
determine Richardson numbers and values of heating
and turbulent diffusivity. Investigation of the intro-
duction of vertical velocities into AFGL model atmo-
sphere codes was undertaken and turbulent diffusion
coefficients were made available for input to these
codes.

ACCESSION for

NTIS   White Section ☑
DDC   B ff Section ☐
UNANNOUNCED   ☐
JUSTIFICATION

BY
DISTRIBUTION/AVAILABILITY CODES
Dist   CIAL

FOREWORD

The program described here consisted of determination of turbulent atmospheric heating rates and diffusion coefficients through microdensitometric reduction and computer analysis of photographs of chemical releases. Related earlier work by the PhotoMetrics research group is described in References 1, 2, and 4.

The author wishes to express his thanks to Mr. Samuel P. Zimmerman (Technical Monitor) of AFGL for his continued encouragement and support, to Dr. P.I. Richards for his assistance in modifying AFGL atmospheric codes, and to Dr. I.L. Kofsky and C.C. Rice who also made important contributions to the studies described in this report.

3

TABLE OF CONTENTS

LIST OF ILLUSTRATIONS

SECTION I

INTRODUCTION

The objective of the program described here is the determination of atmospheric heating rates and turbulent diffusion coefficients from transport and surface brightness distribution of tracer chemical clouds, and incorporation of these values into AFGL model atmosphere codes. Radiance distributions which give mass densities in these artificial clouds are recorded photographically, accessed by microdensitometric scanning, and analyzed by digital computer methods. The primary approach to this problem has been that of analyzing the "turbulent" component of spatial brightness distributions of releases after removing low frequency trends by filtering. The method employs Fourier analysis to determine wavenumber spectra of the higher-frequency fluctuations in scene brightness. These spectral features that characterize turbulence are then analyzed to determine heating rates (rate of dissipation of turbulent kinetic energy) and diffusion coefficients as described in Section II. Additional estimates of heating and diffusion have been derived from measurements of horizontal wind fields in the stratosphere and mesosphere obtained by photographic triangulation methods (Section III). Work with simple AFGL model atmosphere codes is described in Section IV.

A summary of chemical release cloud data analyzed is shown in Table I. The results of these and other analyses were reported as they were completed to AFGL scientists for their immediate use in interpreting atmospheric turbulence phenomena.

Figure 1. Turbulence present in photograph of release Joan
(Wallops I. — 1974) from approximately 90-105 km.

Table 1. Summary of Analyses

Release*	Horizontal Winds	Energy Spectra	Heating Rates	Eddy Diffusion	Shears and Richardson Numbers
XI	No	Yes	Yes	Yes	No
HILDA	No	Yes	Yes	Yes	No
ETTY	No	Yes	Yes	Yes	No
HERTA	No	Yes	Yes	Yes	No
JOAN	No	Yes	Yes	Yes	No
KAM	No	Yes	Yes	Yes	No
WINTER ANOMALY	Yes	No	Yes	Yes	Yes
Stratospheric Trails					
APPOLON	Yes	Yes	Yes	Yes	Yes
FLORA	Yes	Yes	Yes	Yes	Yes
NASA WIND (5 TRAILS)	No	Yes	No	No	No

*Code name of atmospheric chemical release.

SECTION II

DETERMINING ENERGY SPECTRA, HEATING
RATES, AND EDDY DIFFUSION

The methods by which turbulent energy spectra may be calculated
have been treated in Reference 1. Briefly, it is possible to charac-
terize turbulent flow in the atmosphere (Ref's 2-5),whether shear
dominated or buoyancy dominated, by analyzing the surface brightness
distributions of sunlight-scattering or chemiluminescent tracers
released into the atmosphere from rockets. After a short period of
time the chemical reaches pressure equilibrium with ambient species
and conforms to the flow field. Photometrically calibrated photographs
of the release freeze the spatial characteristics of the flow in time and
according to the ergodic hypothesis a scan across this frozen flow
field should be statistically equivalent to the temporal output of a fixed
physical sensor as the flow proceeds across it. A representative
photograph of such turbulence near 100 km (Release Joan – Wallops I.,
1974) is shown in Fig 1.

The actual measurements are made by microdensitometrically
scanning calibrated photographic images of the glow. These photo-
graphic densities may then be converted to scene brightness through
the H&D characteristic of the film and various corrections may be
applied to account for exposure duration, lens T-stop, and varying
sky background (Ref 2).

Precise photogrammetric calibration must also be accomplished
(see next section) to determine the altitude at which the measurements
are performed and the range to the cloud must be known to convert
film plane measurements to distances at the glow. For analyses
requiring time sequences of photographs, correction must be made
for range variation due to cloud movement by the mean wind field.
Turbulent energy spectra are then calculated from the corrected
brightness data either by standard Fourier transform methods or by a

simple summation process ("counting" method – Ref 7) which deter-
mines the energy in wavenumber bands. This method, which is also
described in Ref 1, calculates the energy as the sum and average of
the mean squares of all data fluctuations of length ℓ multiplied by ℓ.
The length ℓ is defined as the distance between zero crossings of the
high pass filtered signal and estimates of power may be calculated at
wavenumbers $k = \pi/\ell$.   This technique is very rapid and provides
reliable spectra in the mid to high wavenumber ranges of interest.
Problems with data truncation and filtering end effects are minimized
(Ref 8). It does require a large amount of input data but this is also
necessary with standard Fourier analysis in order to achieve a desired
statistical accuracy (Ref 9).

Whichever method of calculation is used, correction is performed
for the transfer function of the microdensitometer aperture and for the
modulation transfer function of the microdensitometer itself, which
is dependent upon temporal scanning rate of the instrument. It should
also be noted that <u>true microdensitometer optics</u> (strict control of
light in the transmission microphotometer, and spatial stationarity of
its response) is needed to ensure sufficiently accurate photographic
photometry for these analyses. Flare (scattered) light and nonuniform
sensitivity over the field, present in most full-field-illuminated or
"scanner" type optical systems, may attenuate or nonuniformly reproduce
some of the spatial frequencies present (Ref 10).   Examples of
turbulence spectra calculated for release Joan are shown in Figures
2 and 3.

Determination of heating rates from the spectral (and statistical)
computations may now be accomplished. Specifically, the atmosphere
frequently shows a so-called Kolmogoroff, or inertial spectral range –
a slope indicating minus 5/3-power dependence – that implies, from
dimensional arguments, that turbulent energy is being fed at a constant
rate from large cells into small ones in the subrange of cell dimensions
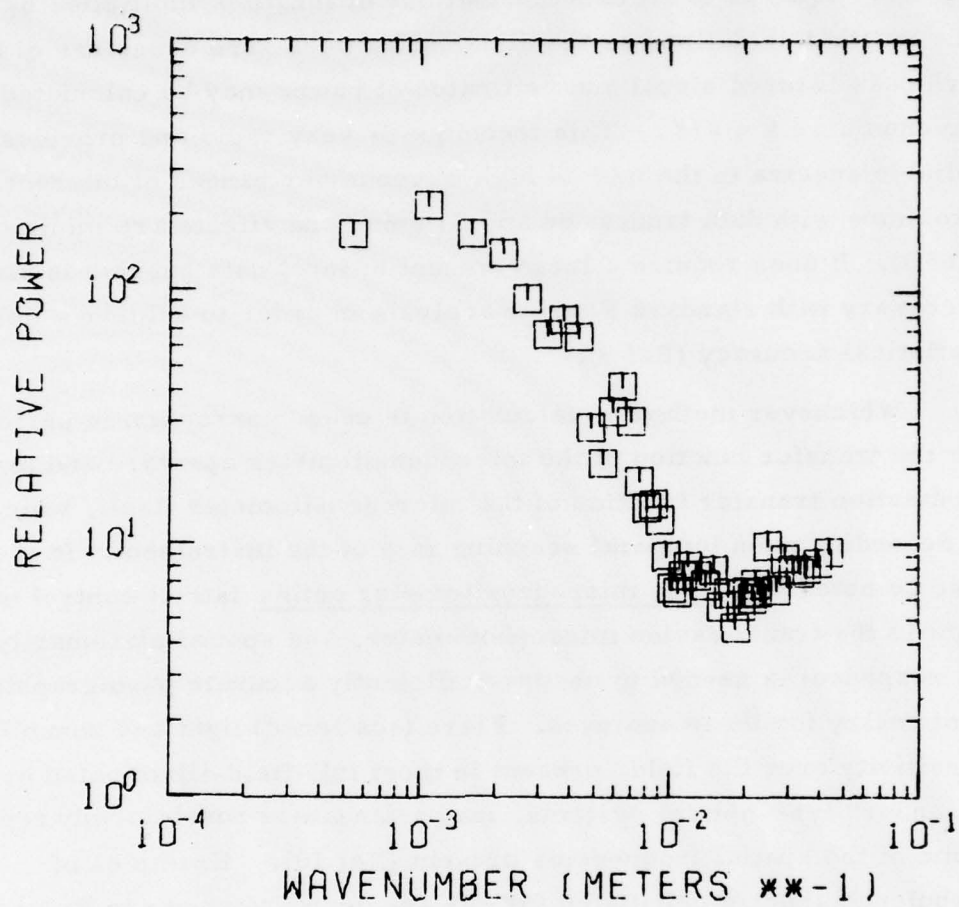in which this slope obtains. Whenever this inertial subrange is

9

Figure 2.   Spectrum of turbulence for release Joan at 92 km
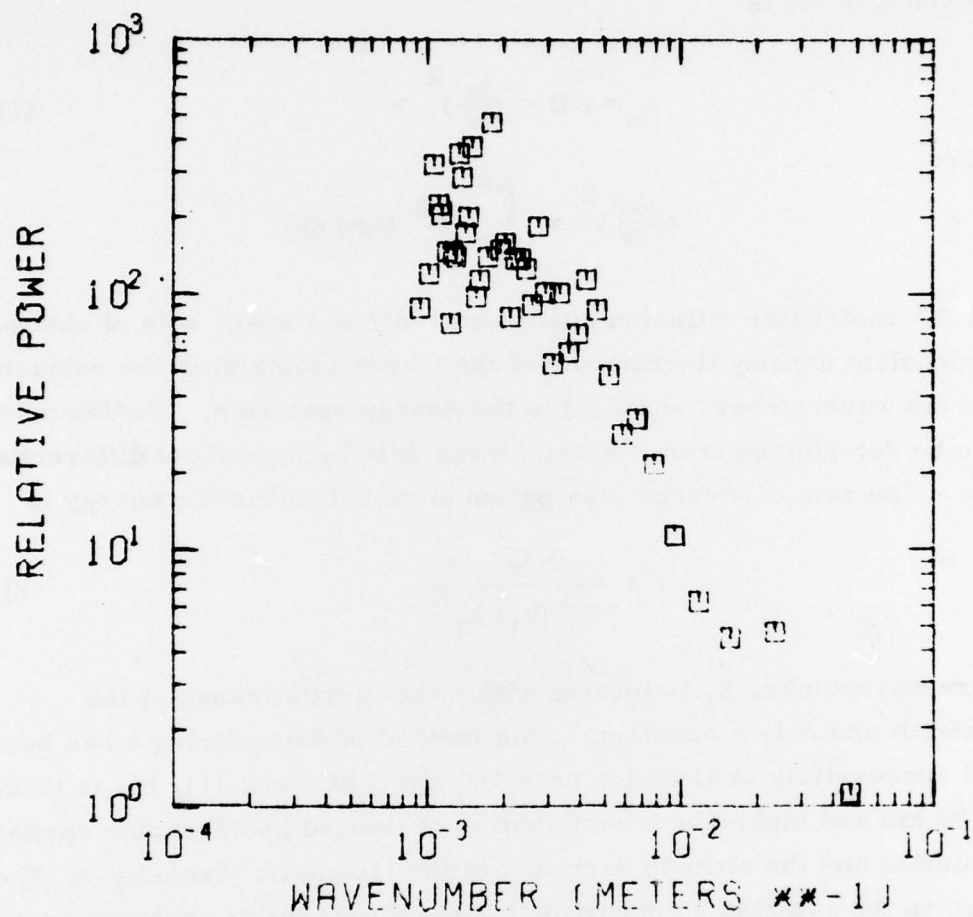determined by standard Fourier analysis.

Figure 3. Spectrum of turbulence for release Joan at 92 km
determined by the "count" method.

11

present the following arguments may be utilized. The scalar rate of decay (ϵ_n) of the density fluctuations (n') due to molecular diffusion at a given altitude is

$$\epsilon_n \approx 6 D < \left(\frac{\partial n'}{\partial x}\right)^2 >$$

(1)

where

$$< \left(\frac{\partial n'}{\partial x}\right)^2 \approx \int_0^\infty k^2 E(k) \, dk$$

and D = molecular diffusion coefficient $\partial n'/\partial x$ = space rate of change of turbulent density fluctuations of the tracer material in the release, k is the wavenumber, and E(k) is the energy spectrum. $\partial n'/\partial x$ may also be determined from the brightness data by numerical differentiation. The rate of viscous dissipation of turbulent kinetic energy is

$$\epsilon = \frac{A \epsilon_n^3}{E^3 (k_1) \, k_1^5}$$

(2)

where wavenumber k_1 is located within the inertial range of the spectrum and A is a constant. This method of determining ϵ has been used successfully at altitudes near 100 km (Ref 5 and 11), but is limited to ~80 km and higher by a combination of limited photographic spatial resolution and the altitude variation of the kinematic viscosity ν. The integrand in the equation 2 approximation for $< (\partial n'/\partial x)^2 >$, behaves as a $k^{1/3}$ to ~0.2 k_ν for the inertial range of E(k), where $k_\nu = (\epsilon /\nu^3)^{\frac{1}{4}}$ is the limiting wavenumber for viscous dissipation. Thus if optical resolution limits the spectrum E(k) to values less than 0.2 k_ν the estimates of $< (\partial n'/\partial x)^2 >$, ϵ_n and ϵ will be low. In existing photographs this will begin to occur roughly at 80 km and grow progressively more severe as ν decreases with altitude. The use of statistically determined $\partial n'/\partial x$ generally underestimates these quantities as well since a portion of the data representative of sky background is retained in the calculation. This relatively smooth data will bias the average of $(\partial n'/\partial x)^2$ toward lower values.

12

Another approach to calculating ϵ may be taken, which goes as follows. The average of the square of the turbulent density fluctuations $\overline{n'^2}$ is calculated for several times. Then

$$\epsilon_n = \frac{\partial \overline{(n'^2)}}{\partial t} \tag{4}$$

and the rate of turbulent dissipation is calculated from equation (3). This formulation for decaying turbulence should be applicable to tracer pulse or trails in any altitude region.

Determinations of eddy diffusion may be accomplished utilizing the turbulent heating rates. It has been shown (Ref 6) than an eddy diffusion coeficient may be expressed as

$$K = C\epsilon^{1/3} k_o^{-4/3} \tag{5}$$

where C is a constant and k_o is the low wavenumber limit of the "inertial" range of the turbulence spectrum. k_o may usually be determined by inspection of the turbulence spectra or calculated from

$$k_o = \ell_o^{-1} = \frac{\int_o^{oo} E(k)\, dk}{\int^{oo} k^{-1} E(k)\, dk}$$

or estimated as $\ell_o \approx C_o (\epsilon/N^3)^{\frac{1}{2}}$ for buoyancy dominated turbulence where ℓ_o is the length scale, C_o = constant, and N = Brunt Vaisala frequency.

Further measurements of heating and turbulent diffusion may be made from knowledge of the atmospheric wind field (Section III), and diffusion may also be determined by using configuration space methods similar to those used for finding molecular diffusion coefficients by measuring the rate of growth of individual cells. Lastly, low frequency energy spectra may be used to calculate wavenumber space halfwidths

13

of clouds which retain some Gaussian character (recall that the
Fourier transform of a Gaussian is also a Gaussian). This last method
may however show very large errors in wavenumber halfwidths and
derived spatial halfwidths due to the photographically limited data
length (and therefore poor resolution of low frequencies).

SECTION III

PHOTOGRAPHIC TRIANGULATION AND VELOCITY TERMINATION

In order to determine quantitative measures of turbulence it is necessary to accurately know the spatial location of the chemical release as a function of time. Over the time of a series of photographic frames required to calculate diffusion coefficients, the wind field in the atmosphere moves the cloud with respect to the camera. This change of range introduces a change in the magnification of the image, and a corresponding change in transverse scale or conversion from image distance to dimensions on the object itself. It is necessary to triangulate to the diffuse glow to find its range and the altitude at which the diffusion is being measured. Methods of determining these photogrammetric calibration factors have improved in accuracy over a period of several years from plane-trigonometric to spherical trigonometric to vector solutions (Ref's 12-16), which provide altitude, latitude, and longitude of points spaced along the trail.

The triangulation process involves determining the triangulation camera orientation from photographs of the stellar background as described in Ref 12. Camera position in latitude, longitude, and altitude above the reference ellipsoid must be known accurately as well as the time of the exposure which records the star positions. Using this time and the known camera position vector equations which relate the measured film plane coordinates of stars to the actual star positions in right ascension and declination may be solved to determine the orientation of the camera optic axis in azimuth and elevation. These relations also allow determination of the precise camera focal length and the rotation about the optic axis (horizonal tilt) needed for registration of the star field with its image.

The next step is to relate the digital film plane positions of the trail as viewed from two photographic sites. These positions may be coordinates of the center line of the trail determined using an automatic

15

scanning microdensitometer, or they may be the coordinates of small dots drawn onto the triangulation negatives in the regions of interest. This latter method, while less accurate, must sometime be used on more turbulent portions of a trail since the automatic scanner would be incapable of defining or following the trail centerline. The methods of Reference 13 together with camera orientations and locations are then used to calculate a line of sight vector for each of the trail points as seen from the two triangulation sites. The best matching of site 1 points with site 2 points is accomplished by minimizing the dihedral angular mismatch between the planes generated by each point line of sight and the line through the two sites. Finally, the positions of matched points in altitude, latitude, and longitude are calculated.

Triangulation accuracy at high altitudes is on the order of 1/4 km, a distance large compared to the object size that results from the film grain on the fast emulsions needed to record the relatively faint clouds; the grain clumping has a scale size of the order of $20\mu m$ (or, one might say, the impulse response of the film is of this order). K-24 cameras, with their 7-inch focal length lenses, image a 25 meter (1/40) spot at a (typical) range of 200 km for a high altitude release, into $\sim 20\mu m$. It is interesting to note in this regard that the resolution of the grainy film sets a limit of about 50 m in the triangulation accuracy that can be achieved with this particular lens. In the lower stratospheric region and with slower films (less grain clumping) the method has produced positional accuracies of $\sim$10 meters. Some problems associated with the method are detailed in Ref 17.

The horizontal wind field may be calculated by analyzing trail motion for several frames typically separated by intervals of 10 to 30 seconds. Velocity components for each altitude are determined by least squares analysis of trail position versus time. At present, the vertical wind component may be calculated only for persistent features which can be uniquely identified not only from time to time but also from at least two sites.

16

These horizontal winds may be used to study in further detail atmospheric turbulence, heating rates, and diffusion. One characterization of turbulence which may be derived from the atmospheric temperature and the wind field is the Richardson number R_i which equals (the Brunt Vaisala frequency)^2 divided by (the vertical shear of the horizontal wind)^2. Richardson number is a measure of the local stability or instability of the atmosphere and its critical value is usually taken as $1/4$; $R_i < 1/4$ indicates instability, $R_i > 1/4$ stability.

Estimates of heating rate may be obtained as the energy deposition rate per unit mass $\epsilon = 1/2 \, \nu(\partial v/\partial z)^2$ where ν = kinematic viscosity and $\partial v/\partial z$ = the vertical shear of the horizontal wind. Profiles of horizontal wind may also be high pass filtered to remove low frequency components revealing the "turbulent" nature of the velocity fluctuations v'. Utilizing the stability criterion R_i heating may be estimated for vertical segments of the trail where R_i remains

$$\epsilon = A < v'^3 > / \ell \tag{6}$$

where ℓ is the segment length and A is a constant of order unity.

For shear dominated turbulence, estimates of vertical diffusivity may be based upon measurement of the horizontal wind and shear. Applying the one dimensional turbulent energy equation

$$K_m(\partial V/\partial Z)^2 - K_n N^2 = \epsilon \tag{7}$$

where K_m is the momentum transfer coefficient, K_h is the heat transfer coefficient, the vertical diffusivity K may be estimated when

$$R_i = N^2/(\partial V/\partial Z)^2 << \tfrac{1}{4} \tag{8}$$

and

$$K_h \approx K_m$$

then

$$K(Z) = \frac{\epsilon}{(\partial V/\partial Z)^2} \approx K_m \tag{9}$$

17

A final estimate of eddy diffusion for buoyancy dominated turbulence may be accomplished using equations 5 and 6 to yield

$$K = < v' > \ell \tag{10}$$

where $< v' >$ is the average turbulent velocity over the vertical segment of length ℓ of the velocity profile. Restrictions on R_i are the same as for equation 6. Dissipation and diffusion derived from equations 6 and 10 are probably underestimated since v' is likely to be underestimated and the ℓ used is certainly smaller than the average scale of the energy containing eddies.

SECTION IV

ATMOSPHERIC MODELING

Modeling of the concentrations of atmospheric constituents has been undertaken over the past few years in an attempt to increase knowledge of the processes which alter atmospheric composition as a function of time and altitude (transport mechanisms, solar heating, photoionization, chemical recombination). Computer modeled profiles of species may be compared to observed concentrations to assess the models' success.

These models have become increasingly complex as they are extended to account for as many known mechanisms and even very minor ionic species as computer capability will allow. Serious questions have been raised (Ref 18) about the near universal application of the assumption of diffusive equilibrium which dictates a virtually static state for individual species above the turbopause. Additionally, modeled variation of turbopause height may greatly effect species concentrations above the turbopause (Ref 19). It has been demonstrated (Ref 20) that the neutral temperature profile strongly depends upon the eddy diffusion coefficient (heat transport due to eddy conduction), and scale heights of species are affected by variation in K (by mixing) and by changes in production and loss rates (by changes in neutral temperature). The general use of time invariant profiles for eddy diffusion and temperature in the solution of the system of mass and momentum conservation equations must receive further attention.

AFGL model codes for simple nonreactive atmospheres (Argon-nitrogen, Kryton-nitrogen) were modified to introduce transport due to diurnally varying vertical winds. Early attempts to execute this code terminated when winds removed all material from one or more altitudes. Several factors leading to this condition were identified and some of the problems corrected.

19

The first major problem identified as an inherent instability in the one-sided differencing techniques used (briefly described in Appendix A). This was remedied by instituting an offset in the location of action of velocities and fluxes – number densities and temperature refer to the center of an altitude cell whereas velocities and fluxes refer to the upper boundary of the cell. Successful introduction of vertical winds must also be done slowly – the wind increasing to maximum values only after the iterative solution to achieve diurnally reproducible species concentration profiles has executed several diurnal cycles.

A simplified solution to allow variation of mean mass and temperature (energy balance equation) was tested and found inadequate. The theoretical solution for the full mass motion case was derived but not implemented because of the considerable code modification that would be necessary. Efforts were also made to reduce execution time of the code by optimizing certain calculations and by exploring how to increase the time step or the altitude increment.

The final diurnally reproducible species number density profiles obtained with the inclusion of vertical winds had differences and inconsistencies with experimental results probably attributable to partial nature of the code solutions, since some parameters known to vary diurnally are still treated as time-independent.

SECTION V

CONCLUSIONS AND RECOMMENDATIONS

Present techniques of spectral analysis are an effective means of determining energy spectra representative of atmospheric turbulence from photographic records of chemical releases. These spectra allowed calculations of turbulent atmospheric heating rates and turbulent diffusion coefficients which were used as input to computer codes that model the behavior of atmospheric species. Additional measurement of heating and diffusion were derived from the horizontal winds obtained by triangulation methods from these same photographs. Large volumes of data were analyzed, which were reported in whole or in summary form to AFGL scientists as the results were obtained.

Further improvements in modeling procedures depend upon incorporating an energy balance equation to allow use of time dependent profiles for temperature, eddy diffusivity and vertical winds; extension of the codes to three spatial dimensions must also consider mean horizontal wind motions. Adequate assessment of the performance of more comprehensive models incorporating these time varying quantities requires further experimental investigation, especially of eddy diffusivity about which the least is known. The hundreds of existing films of chemical releases taken over several years can be utilized to systematically study both altitude and diurnal variations of winds, heating rate, and eddy diffusion especially at altitudes below 120 km where turbulent mixing and heating predominate.

REFERENCES

1. C.A. Trowbridge, I.L. Kofsky, Densitometric Analysis to Determine Artificial Cloud Expansion Characteristics, AFCRL-TR-75-0147, 14 Mar 1975.

2. I.L. Kofsky, C.A. Trowbridge, R.H. Johnson, Analysis of Chemical and Smoke Releases in the Atmosphere, AFCRL-TR-74-0102, 31 Jan 1974.

3. S.P. Zimmerman, J. Appl. Meteorol. 4, 279 (1965).

4. C.A. Trowbridge, I.L. Kofsky, and R.H. Johnson, "Measurement of Turbulence and Diffusion in High-Altitude Chemical Clouds," AFCRL-68-0382, 30 July 1968.

5. S.P. Zimmerman and C.A. Trowbridge, The Measurement of Turbulent Spectra and Diffusion Coefficients in the Altitude Region 95 to ~110 km, Space Research XII (1973).

6. S.P. Zimmerman and N.V. Loving, Turbulent Dissipation and Diffusivities in the Stratosphere, CIAP-DOT, Volume 1, The Natural Stratosphere (1974).

7. S.P. Zimmerman, Turbulence Observed in Electron Density Fluctuations in Equatorial E Region over Thumba, India, JGR, 81, Oct 1976.

8. S.P. Zimmerman, A.F. Quesada, V.L. Corbin, C.A. Trowbridge, R. Olsen, Dept of Transportation, CIAP Sponsored Research, Final Report.

9. P.I. Richards, Computing Reliable Power Spectra, IEEE Spectrum, 4, January 1967.

10. I.L. Kofsky, Reduction of Pictorial Data by Microdensitometry, Chapter in book "Aerospace Measurement Techniques," NASA SP-132, January 1967.

11. S.P. Zimmerman, N.W. Rosenberg, A.C. Faire, D. Golomb, E.A. Murphy, W.K. Vickery, C.A. Trowbridge, and D. Rees, The Aladdin II Experiment: Part I, Dynamics, Space Research XIV (1974).

12. A.F. Quesada, Vector Evaluation of Triangulation Camera Parameters from Star Photographs, AFCRL-TR-75-0451, 21 Aug 1975.

13.   A. F. Quesada, Application of Vector and Matrix Methods to Triangulation of Chemical Releases in the Upper Atmosphere, AFCRL-71-0233, 23 April 1971.

14.   H. B. Tolefson, R. M. Henry, A Method of Obtaining Detailed Wind Shear Measurements for Application to Dynamic Response Problems of Missile Systems, JGR, 66, 2849-2862, 1961.

15.   D. L. Albritton, L. C. Young, H. D. Edwards, J. L. Brown, Position Determination of Artificial Clouds in the Upper Atmosphere, Photogrammetric Eng. 28, 608, Sept 1962.

16.   H. D. Edwards, Study of Photochemistry, Physical State and Motion of the Upper Atmosphere, Final Report AFCRL-63-488, March 1963.

17.   C. A. Trowbridge, I. L. Kofsky, Ronald H. Johnson, Recording and Analysis of Optical Data from Stratospheric Dynamics Experiments, AFGL-TR-78-0015, 14 January 1978.

18.   S. P. Zimmerman, T. J. Keneshea, The Thermosphere in Motion, JGR 81, 1 July 1976.

19.   J. D. George, S. P. Zimmerman, and T. J. Keneshea, "The Latitudinal Variation of Major and Minor Neutral Species in the Upper Atmosphere," Space Research XII (1972).

20.   S. Chandra and A. K. Sinha, The Role of Eddy Turbulence in the Development of Self Consistent Models of the Lower and Upper Thermosphere, Journal of Geophysical Res. 79, 13 (1974).

APPENDIX A
MEMORANDUM

DATE: June 1975

TO: T. Keneshea

FROM: P. I. Richards

SUBJECT: Instability of One-Sided Differencing

In simple terms, a set of equations such as

$$\frac{\partial u}{\partial t} + \alpha u = - \frac{\beta}{n} \frac{\partial n}{\partial z}$$
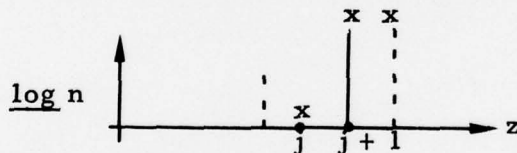
$$\frac{\partial n}{\partial t} = - \frac{\partial}{\partial z} (nu)$$

Leads to relations such as

$$U_j^{\ell + 1} = aU_j^{\ell} - \frac{b}{n_j} \left(\frac{n_{j+1} - n_j}{\Delta z} \right)$$

if one-sided differences are used.

Now suppose a situation like the following develops

where n_{j+1} is very much larger than n_j. This leads quite properly to a large negative $U_j^{\ell + 1}$, BUT this U_j applies to cell j, and its effect is to further empty cell j. If $U_{j-1}^{\ell + 1}$ in cell j - 1 is not equally large and positive (as it may well not be), n_j decreases still further, making the next $U_j^{\ell + 2}$ even more negative, and the situation runs away.

24